Thin-Plate Spline Radial Basis Function Scheme for Advection-Diffusion Problems

I. Boztosun [1 2], A. Charafi [1], M. Zerroukat [3], and K. Djidjeli [4]

[1] *Department of Physics, Erciyes University, Kayseri 38039 Turkey.*
[2] *Computational Mathematics Group, University of Portsmouth, Portsmouth PO1 2EG, United Kingdom.*
[3] *NWP Division, Meteorological Office, London Road, Bracknell, Berkshire RG12 2SZ, United Kingdom.*
[4] *Department of Ship Science, University of Southampton, Highfield, Southampton SO17 1BJ, United Kingdom.*

Abstract

We present a meshless method based on thin plate radial basis function method for the numerical solution of advection-diffusion equation, which has been a long standing problem. The efficiency of the method in terms of computational processing time, accuracy and stability is discussed. The results are compared with the findings from the finite difference methods as well as the analytical solution. Our analysis shows that the radial basis functions method, with its simple implementation, generates excellent results and speeds up the computational processing time, independent of the shape of the domain and irrespective of the dimension of the problem.

Keywords: Meshless Methods, Radial Basis Functions, Thin Plate Spline, Finite Difference Method, Partial Differential Equation, Linear Advection-Diffusion Problem

1 Introduction

The solution of the advection-diffusion equation is a long standing problem and many numerical methods have been introduced to model accurately the interaction between advective and diffusive processes. This modelling is the most challenging task in the numerical approximation of the partial differential equations [1] and the available numerical solutions are very sophisticated in order to avoid two undesirable features: oscillatory behavior and numerical diffusion, which are mainly due to the advection term when it dominates (see also Brebbia *et. al.* [2, 3], Partridge *et. al.* [4, 5] for a detailed discussion).

In general, the numerical solution of advection-diffusion equations has been dominated by either Finite Difference, Finite Element or Boundary Element Methods. These methods are derived from local interpolation schemes and require a mesh to support the application. It is well known that Finite Difference and Finite Element solutions of the advection-diffusion equation present numerical problems of oscillations and damping. On the other hand, boundary element solutions seem to be relatively free from these problems, as shown by Brebbia and Skerget [3].

The numerical solution of this equation is a difficult task because of two reasons; Firstly, the nature of the governing equation, which includes first-order and second-order partial derivatives in space. According to the value of κ (diffusion coefficient) and v (advection coefficient), the equation becomes parabolic for diffusion dominated processes or hyperbolic for advection dominated processes. Traditional finite difference methods are generally accurate for solving the former but not the latter, in which case oscillations and smoothing of the wave front are introduced. This can be interpreted as the artificial diffusion intrinsic to these methods [3, 4, 5, 6, 7, 8]. Secondly, since the above-mentioned numerical methods are all mesh dependent, it is vital to construct an appropriate mesh to obtain a better approximation to the problem. However, the construction of an appropriate mesh is not an easy task and sometimes the problems cannot be solved because of the lack of an appropriate mesh structure [1, 9, 10, 11, 12, 13].

Because of the complexity of mesh-generation, considerable effort has been devoted in recent years to the development of mesh-free methods, also called meshless methods. These methods aim to eliminate the structure of the mesh and approximate the solution using a set of quasi-random points rather than points from a grid discretization.

In this paper, we conduct a comparative study of mesh free and mesh dependent methods. Radial Basis Functions (RBF) as a mesh free method is examined and the results are compared with the findings of Finite Difference Method (FDM) and analytical solution. In the next section, we introduce the advection-diffusion equation and its applications. Then, we briefly introduce a meshless scheme based on Thin Plate Spline (TPS) radial basis function method. In section 4, we describe the solution of this equation using finite difference method in order to make a comparison between the mesh-free and mesh-dependent methods. Section 5.1 shows the findings of our analysis and finally, we conclude in section 6.

2 Advection-Diffusion Equation

The advection-diffusion equation can be written in the following form:

$$\frac{\partial u(\mathbf{x},t)}{\partial t} = \kappa \nabla^2 u(\mathbf{x},t) + \mathbf{v} \cdot \nabla u(\mathbf{x},t), \qquad \mathbf{x} \in \Omega \subset \mathbf{R}^d, t > 0 \tag{1}$$

Together with the general boundary and initial conditions

$$c_1 u(\mathbf{x},t) + \mathbf{c}_2 \cdot \nabla u(\mathbf{x},t) = f(\mathbf{x},t), \qquad \mathbf{x} \in \partial\Omega, t > 0 \tag{2}$$

$$u(\mathbf{x},t) = u_0(\mathbf{x}), \qquad t = 0 \tag{3}$$

where $u(\mathbf{x},t)$ is the temperature at the position $\mathbf{x}$ at time t, $\mathbf{x} = (x_1, x_2, \ldots, x_d)$ is the vector position, d is the dimension of the problem, ∇ the gradient differential operator, Ω is a bounded domain in $\mathbf{R}^d$, $\partial\Omega$ the boundary on Ω, κ the diffusion coefficient, $\mathbf{v} = [v_x, v_y, v_z]^T$ the advection coefficient or velocity vector, c_1 and $\mathbf{c}_2$ are known constants, and $f(\mathbf{x},t)$ and $u_0(\mathbf{x})$ are known functions.

A large number of problems in physics, chemistry and other branches of science can be modelled by the advection-diffusion equation. For example, the steady-state distribution of a passive substance dissolved in water and transported by the flow, transport of multiple reacting chemicals, the dispersion of atmospheric tracers or the far-field transport of decaying radionuclides through a porous medium can all be described by the advection-diffusion equation.

Industrial problems involving the solution of the advection-diffusion equations range from the solution of fluid dynamic problems such as the galvanization of steel sheets and alloy solidification, heat transfer applications such as the temperature increase in current carrying wires, the water jet cooling of a moving hot rolled steel strip, to financial applications such as the variation of asset prices in stock-market.

3 Radial Basis Function Approximation

The approximation of a function $u(\mathbf{x})$, using RBF, may be written as a linear combination of N radial functions:

$$u(\mathbf{x}) \simeq \sum_{j=1}^{N} \lambda_j \phi(\mathbf{x}, \mathbf{x}_j) \qquad for \ \mathbf{x} \in \Omega \subset \mathbf{R}^d \tag{4}$$

where N is the number of data points, λ's are the coefficients to be determined and ϕ is the radial basis function.

We use the Thin Plate Spline RBF in our analysis. The reason is that previous analyses have shown that the MultiQuadrics (MQ) and Thin Plate Spline (TPS) give the most accurate results for scattered data approximations [14]. However, the accuracy of the MQ method depends on a shape parameter and as yet there is no mathematical theory about how to choose its optimal value . Hence, most applications of the MQ use experimental tuning parameters or expensive optimization techniques to evaluate the optimum shape parameter [15]. While the TPS method gives good agreement without requiring such additional parameters and based on sound mathematical theory [16].
An mth order TPS is defined as

$$\phi(\mathbf{x},\mathbf{x}_j) = \phi(r_j) = r_j^{2m} log(r_j), \qquad m = 1, 2, 3, \ldots \tag{5}$$

where $r_j = \|\mathbf{x} - \mathbf{x}_j\|$ is the Euclidean norm. Since ϕ is C^{2m-1} continuous, a higher-order TPS must be used, for higher-order partial differential operators. The advection-diffusion equation is of second-order, m=2 is used to ensure at least C^2 continuity for u.

The collocation of equation (4) at N points results in a system of linear equations, which is solved using Gaussian elimination with partial pivoting in order to determine the coefficients $(\lambda_1, \ldots, \lambda_N)$.

4 Solution with FD and RBF Methods

Equation (1) is discretized using Crank-Nicholson (θ-weighted) method

$$\begin{aligned} u(\mathbf{x}, t+\triangle t) - u(\mathbf{x}, t) &= \triangle t\theta \left(\kappa \nabla^2 u \mid_{t+\triangle t} + \mathbf{v} \cdot \nabla u \mid_{t+\triangle t}\right) \\ &+ \triangle t(1-\theta)\left(\kappa \nabla^2 u \mid_t + \mathbf{v} \cdot \nabla u \mid_t\right) \end{aligned} \tag{6}$$

where $0 \leq \theta \leq 1$, and $\triangle t$ is the time step size. Using the notation, $u^n = u(\mathbf{x}, t^n)$ where $t^n = t^{n-1} + \triangle t$, equation (6) can be written as

$$u^{n+1} + \alpha \nabla^2 u^{n+1} + \beta \cdot \nabla u^{n+1} = u^n + \eta \nabla^2 u^n + \xi \cdot \nabla u^n \tag{7}$$

where

$$\alpha = -\kappa\theta\triangle t \qquad \beta = [\beta_x, \beta_y, \beta_z]^T = -\theta \triangle t \mathbf{v} \tag{8}$$

and

$$\eta = \kappa \triangle t(1-\theta) \qquad \xi = [\xi_x, \xi_y, \xi_z]^T = \triangle t(1-\theta)\mathbf{v} \tag{9}$$

We define the new operators H_+ and H_- by

$$H_+ = 1 + \alpha \nabla^2 + \beta \cdot \nabla, \qquad H_- = 1 + \eta \nabla^2 + \xi \cdot \nabla \tag{10}$$

In the FDM, the operators H_+ and H_- are discretized by using the second-order central difference for the diffusion terms and backward difference for the advection terms. In the RBF method, the function u is approximated by a linear combination of radial functions as in equation (4), and the operators H_+ and H_- are applied to the approximation. The time-discrete equation (6) becomes

$$H_+ u^{n+1} = H_- u^n \tag{11}$$

To be able to compare the FDM and RBF approaches, we use the same grid (discretization in space) and assume $\mathbf{x}(x_i, y_i)$ for $i = 1, \ldots, N$ to be a set of discrete points that defines a uniform grid with $\triangle x$ and $\triangle y$ being the step size in the x- and y-directions respectively.

4.1 Finite Difference Method

In the FDM, the Laplacian and gradient operators are discretized using the second-order central difference and backward difference respectively. When the FD approximations are substituted in the operators H_+ and H_-, the boundary and initial conditions are applied, and the equations are re-arranged, we obtain a symmetric system of linear equations, which is solved using Gaussian elimination with partial pivoting to get an estimate of $u(\mathbf{x}, t)$.

4.2 Radial Basis Function Method

In contrast to FDM, in RBF method, we never discretize the differential operators, instead the operators are applied to the basis functions directly.

That is, if we assume that there are a total of N collocation points (called also centers), $u(\mathbf{x}, t^n) = u(x, t^n)$ is approximated by:

$$u^n(\mathbf{x}) \simeq \sum_{j=1}^{N} \lambda_j^n \varphi(r_j) \tag{12}$$

where r_j is the Euclidian distance between the points $\mathbf{x}$ and $\mathbf{x}_j$. To determine the interpolation coefficients $(\lambda_1, \lambda_2, \ldots, \lambda_{N-1}, \lambda_N)$, the collocation method is used by applying (12) at every point $i = 1, \ldots, N$, giving:

$$u^n(x_i) \simeq \sum_{j=1}^{N} \lambda_j^n \phi(r_{ij}), \qquad i = 1, \ldots, N \tag{13}$$

where $r_{ij} = \sqrt{(x_i - x_j)^2}$. Since the radial basis functions method depends only on the relative distance between the nodes, it is easy to extend this method to the higher dimensions by just taking the relative distance r as $r_{ij} = \sqrt{(x_i - x_j)^2 + (y_i - y_j)^2 + (z_i - z_j)^2}$.

The operators H_+ and H_- are applied to the approximation (12) to get:

$$\sum_{j=1}^{N} \lambda_j^{n+1} H_+ \phi(r_{ij}) = \sum_{j=1}^{N} \lambda_j^{n} H_- \phi(r_{ij}), \qquad i = 1, \ldots, N \tag{14}$$

The above equation is applied at every point $i = 1, \ldots, N$. In order to determine the interpolation coefficients $(\lambda_1, \lambda_2, \ldots, \lambda_N)$, the Gaussian elimination method with partial pivoting is used and the λ's are back-substituted to get an approximation of $u(x,t)$.

5 Numerical Examples

5.1 Example 1

For the comparison of TPS-RBF and FDM solutions, consider following one-dimensional problem with its analytical solution. It consists of a Dirichlet problem defined as:

$$\frac{\partial u(x,t)}{\partial t} = \kappa \frac{\partial^2 u(x,t)}{\partial x^2} - v \frac{\partial u(x,t)}{\partial x} \tag{15}$$

$$u(0,t) = ae^{bt}, \;\; u(6,t) = ae^{bt+6c}, \;\; t > 0 \tag{16}$$

$$u(x,0) = ae^{cx} \tag{17}$$

The analytical solution is given by

$$u(x,t) = ae^{bt+cx} \quad and \quad c = \frac{v \pm \sqrt{v^2 + 4\kappa b}}{2\kappa} > 0 \tag{18}$$

We have made an extensive investigation of this equation by considering many different values of κ and v. We have observed that FDM and RBF solutions are in perfect agreement with the analytical solution for the diffusion dominated problems. This is demonstrated in Figure 1. However, for the advection dominated calculations, FD method shows spurious oscillatory structure whereas RBF approximation gives excellent agreement with the exact solution. As it is well known, finite difference methods are generally accurate for solving the diffusion dominated cases but not the advection dominated ones [4]. The reason for this inaccuracy might be due to the artificial diffusion introduced by the numerical approximation. We know that the error term in the backward or upwind difference method has the even (second) derivative as the dominant term since the method is first-order accurate and even derivatives are associated with dissipation errors. Thus sharp gradients within the solution are smeared, resulting in an inaccurate solution.

The results of these advection dominated calculations are shown in Figures 2 and 3. The linear damping of the disturbance as it is marched forward in the x-direction in Figure 2 and Figure 3 is clearly due to the numerical problems associated with the method. The disagreement between FDM and analytical solution becomes clear at large distances and the error increases with time. As it is clearly seen from these figures, FDM results at large distances blow up because of the artificial diffusion created by the domination of the advection term.

In order to increase the accuracy for FDM, one can do grid refinement. However, this also involves computationally intensive and expensive operations, and may not be possible in many cases. Thus, it is desirable to increase accuracy by employing higher order finite difference equations. These different analyzes are very significant when extracting information from physical system under consideration without any numerical accuracy problem. The interpretation of such physical phonema using FDM as shown in Figures 2 and 3 may be completely misleading otherwise.

We see from Figures 2 and 3, where FDM fails, that RBF method gives excellent agreement with the analytical solution. In these calculations, the importance of the RBF method becomes apparent. The numerical results show that RBF based meshless schemes achieve comparable results as other mesh-based methods such as finite differences and DRM. Furthermore, they are remarkably simple, especially for complicated domains and higher dimensions.

5.2 Example 2

As a second example, we investigate following linear advection-diffusion equation in two dimensions:

$$\frac{\partial u}{\partial t} = \kappa_x \frac{\partial^2 u}{\partial x^2} + \kappa_y \frac{\partial^2 u}{\partial x^2} + v_x \frac{\partial u}{\partial x} + v_y \frac{\partial u}{\partial y} \tag{19}$$

Together with the Dirichlet type boundary and initial conditions

$$\begin{aligned} u(0,y,t) &= ae^{bt}(1+e^{-c_y y}), \;\; u(1,y,t) = ae^{bt}\left(e^{-c_x} + e^{-c_y y}\right) \\ u(x,0,t) &= ae^{bt}(1+e^{-c_x x}), \;\; u(x,1,t) = ae^{bt}\left(e^{-c_x x} + e^{-c_y}\right) \;\; t > 0 \end{aligned} \tag{20}$$

$$u(x,y,0) = a\left(e^{-c_x x} + e^{-c_y y}\right) \tag{21}$$

The analytical solution is given by

$$\begin{gathered} u(x,y,t) = ae^{bt}\left(e^{-c_x x} + e^{-c_y y}\right) \\ c_x = \frac{v_x + \sqrt{v_x^2 + 4b\kappa_x}}{2\kappa_x} \quad \textit{and} \quad c_y = \frac{v_y + \sqrt{v_y^2 + 4b\kappa_y}}{2\kappa_y} \end{gathered} \tag{22}$$

This equation is solved using TPS and FDM with 121 points on an equivalent grid system. The results are shown in Figures 4 and 5 and compared with the analytical solution. The TPS and FDM are in perfect agreement with the analytical solution for low Péclet numbers. However, when advection dominates, we observe that, as in the case of one-dimensional calculations, FDM becomes unstable and produces large errors. The RBF method generates better agreement with the analytical solutions with respect to FDM.

We also examined the effect of the number of nodes in the calculations. If we increase the number of nodes, as expected the error gets smaller and smaller. This is illustrated in Figure 6 with filled-circles for the two-dimensional case. The solid lines in the same figure is obtained from the logarithmic fit of the curves. From this figure, it can be seen that when the number of nodes starts increasing FDM and RBF solutions converge.

As regards the computational speed of the two methods, RBF method can be thought slower than FDM due to the fact that RBF method generates a fully-populated matrix, whereas FD method generates a symmetric tridiagonal matrix. However, when comparing the two methods for a given accuracy RBF method is much faster than FDM. This is illustrated in Figure 6. For a given accuracy, say 0.006, RBF method requires ≈ 100 nodes and a CPU time of 1.6 seconds (it takes 0.28 seconds for the FDM to compute the solution for the same number of nodes). But in order to achieve the same accuracy with FDM, we need between 500 and 700 nodes and the calculations require 60.8 seconds for 529 nodes and 357.3 seconds for the 676 nodes. This clearly demonstrates that RBF method is much faster than traditional methods for a given accuracy.

6 Conclusion

We have presented and discussed the solution of advection-diffusion equation using RBF and FD methods. The solution of advection-diffusion equation has been a difficult task for all numerical methods because of the nature of the governing equation. According to the value of κ and v, the equation becomes parabolic (for diffusion dominated processes) or hyperbolic (for advection dominated processes). Traditional finite difference methods are generally accurate for solving the former but not the latter, in which case oscillations and smoothing of the wave front are introduced. This can be interpreted as the artificial diffusion intrinsic to these methods.

However, as shown in this paper RBF method does not introduce such artifial effect and it is not important for the RBF method whether the process is advection/convection or diffusion dominated. From application viewpoints, the implementation of RBF method is very simple and straightforward, irrespective of the dimension of the problem and the shape of the domain under consideration. As our numerical results show, they achieve similar results as more complicated grid/mesh methods such as finite differences method and work when the latter fails.

Acknowledgments

I. Boztosun would like to thank EPSRC for their financial support and members of the Porstmouth University for their hospitality during his stay.

References

[1] Morton KW, Numerical Solution of Convection-Diffusion Equation, Chapman & Hall (1996).

[2] Boztosun I and Charafi A, RBF-based Meshless Schemes for Advection-Diffusion Problems, Advances in Boundary Element Techniques II (2001) 573.

[3] Brebbia CA and Skerget L, Time Dependent Diffusion Convection Problems Using Boundary Elements, Numerical Methods in Laminar and Turbulent Flow III, Pineridge Press, Swansea, 1983.

[4] Partridge PW, Brebbia CA and Wrobel LC, The Dual Reciprocity Boundary Element Method (1991).

[5] Ikeuchi M and Onishi K, Boundary Element Solution to Steady Convective Diffusion Equations, Applied Mathematical Analysis, Vol. 7, No. 2, 115 (1983).

[6] Roache PJ, Computational Fluid Dynamics, Hermosa Publishers, Albuquerque, New Mexico, USA (1972).

[7] Hughes TJR (Ed.), Finite Element Methods for Convection Dominated Flows, ASME AMD-Vol. 34, New York, USA (1979).

[8] Zerroukat M, Power H and Chen CS, A numerical method for heat transfer problems using collocation and radial basis functions, Int. J. Numer. Meth. Eng. **42**, 1263 (1998).

[9] Kansa EJ, Multiquadrics: A scattered data approximation scheme with applications to computational fluid-dynamics, Computational Mathematics and Applications 19, 147 (1990).

[10] Tveito A and Winther R, Introduction to Partial Differential Equations: A Computational Approach, Springer (1998).

[11] Morton KW and Mayers DF, Numerical Solution of Partial Differential Equations, Cambridge University Press (1996).

[12] Schaback R, Lecture notes on Reconstruction of Multivariate Functions from Scattered Data (1997).

[13] Thomas JW, Numerical Partial Differential Equations: Finite Difference Methods, Springer (1995).

[14] Franke R, Scattered data interpolation: test of some methods, Mathematics of Computation 38, 181 (1982).

[15] Carlson RE and Foley T, The parameter R^2 in multiquatric interpolation, Computational Mathematics and Applications 21, 29 (1991).

[16] Duchon J, Splines minimizing rotation-invariant semi-norms in Sobolev spaces, Constructive Theory of Functions of Several variables, Lecture Notes in Mathematics, Vol. 38, Schempp W, Zeller K (eds). Springer: Berlin, 85 (1977).

[17] van Genuchten M and Alves WJ, Analytical Solution of the one-dimensional Convective-Dispersive Solute Transport Equation, U.S. Department of Agriculture, Tecnical Bulletin No. 1661, Washington (1982).

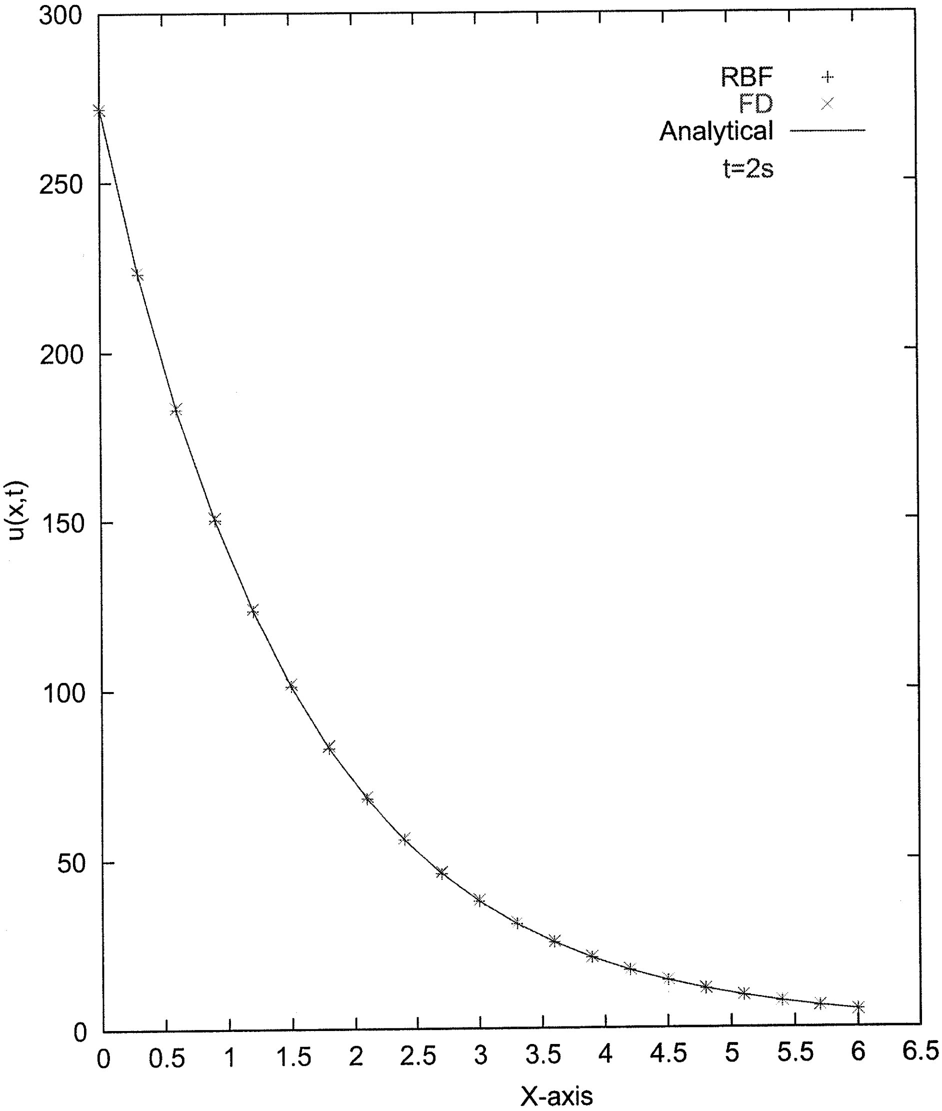

Figure 1: Example-1: Comparison of FDM and RBF solutions with the analytical one for the diffusion dominated calculation, $\kappa = 1.0$ and v=0.1.

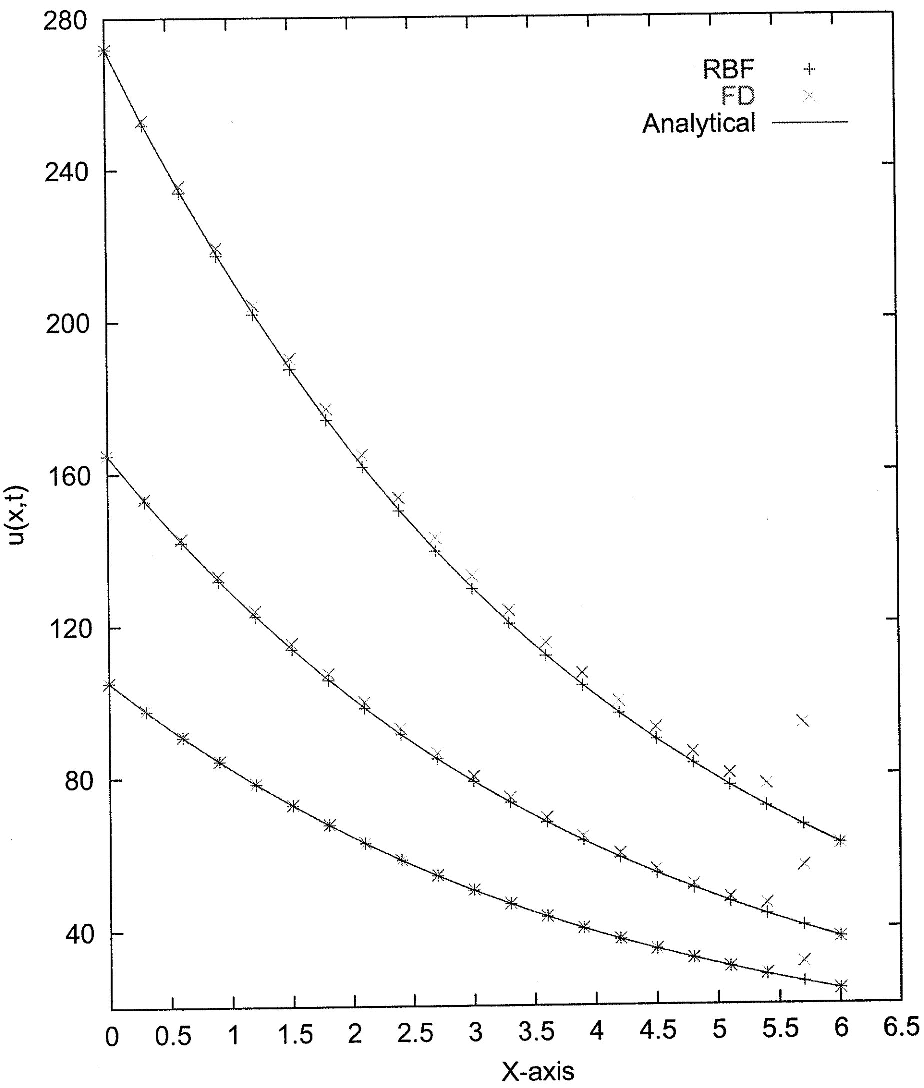

Figure 2: Example-2: Comparison of FDM and RBF solutions with the analytical one, $\kappa = 2$ and v=1 at times (from below) t=0.1s, 1.0s and 2s.

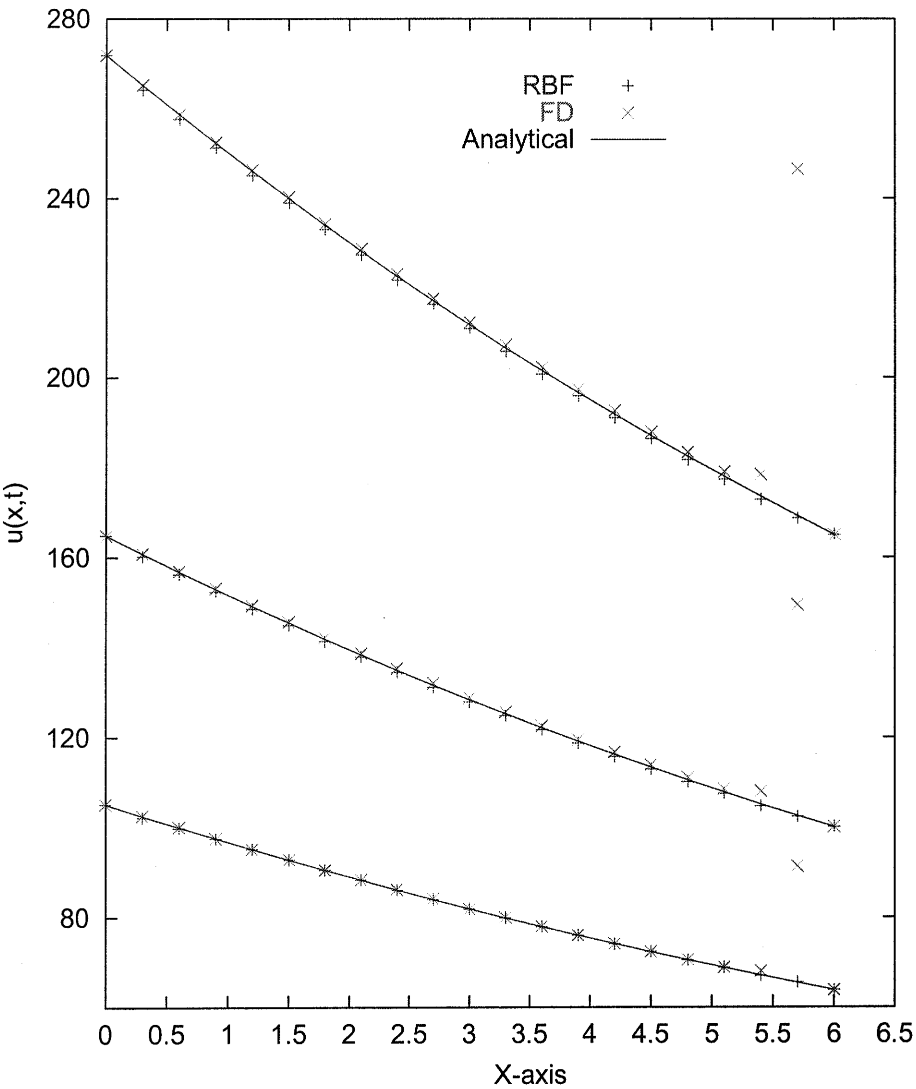

Figure 3: Example-2: Comparison of FDM and RBF solutions with the analytical one, $\kappa = 6$ and v=1 at times (from below) t=0.1s, 1.0s and 2s.

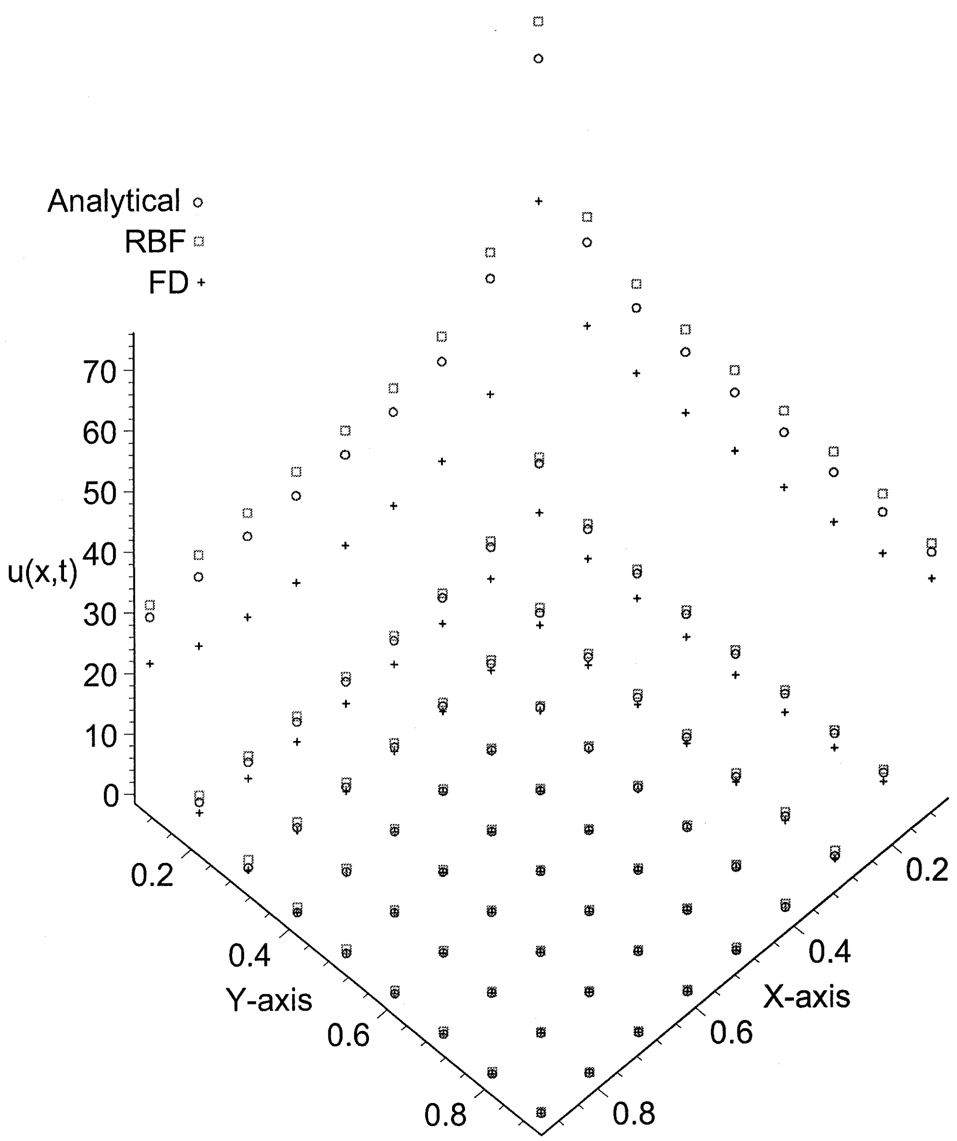

Figure 5: Example-3: Comparison of FDM and RBF solutions with the analytical one, v_x=0.1, v_y=0.1, κ_x=1.4, κ_x=1.7.

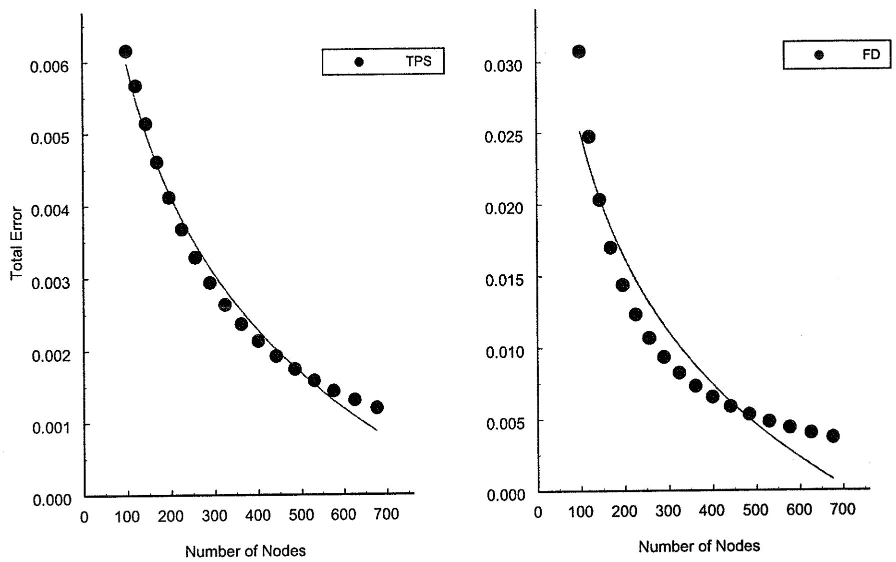

Figure 6: Variation of the total error with the number of nodes for RBF and FDM at time t=1.0s.